Electronic Supplemental Information

Multistep soft chemistry method for valence reduction in transition metal oxides with triangular (CdI_2-type) layers

Colin K. Blakely,[a] Shaun R. Bruno,[a] Viktor V. Poltavets*[a]

[a] Department of Chemistry, Michigan State University, East Lansing, Michigan, 48824, USA

Full Experimental Methods

All compounds were prepared in a nitrogen filled glovebox then transported to a furnace in a sealed alumina tube. NaOH (Alfa Aesar, 99%), Na_2CO_3 (Sigma Aldrich, 99.9%), Br_2 (Jade Chemical, ACS Grade), I_2 (Jade Chemical, ACS), Co_3O_4 (Alfa Aesar, 99.99%), α-Fe_2O_3 (Strem Chemical, 99.98%), Na metal (Mallinckrodt, ACS Grade), n-BuLi (Sigma Aldrich, 1.6 M in hexanes) and benzophenone (Sigma Aldrich, 99%) were used as received without further purification. $Ca(NO_3)_2 \bullet 4H_2O$ (Sigma Aldrich, 99.9%) was thermally treated at 500 °C in dry air for 2 hours to afford anhydrous $Ca(NO_3)_2$.

Synthesis of Na_xCoO_2 phases 1.600g (40 mmol) NaOH and 2.63g (10.91 mmol) Co_3O_4 were ball milled for 30 minutes, then fired at 500 °C for 120 hours under O_2, affording pure phase $NaCoO_2$ after washing out excess of NaOH with anhydrous methanol. $Na_{0.74}CoO_2$ was prepared by heat treatment of mixture of 1.908g (18 mmol) Na_2CO_3 with 3.77g (15.66 mmol) Co_3O_4, for 48 hrs at 850 °C under O_2 flow. The more oxidized cobaltates (x = 0.50, 0.34) were synthesized in 5g batches by room temperature reaction with a 10 molar excess of I_2 and Br_2 in acetonitrile for 96 hrs and 108 hrs, respectively. The NaI/NaBr was removed by washing with dry acetonitrile. $Na_{0.74}CoO_2$ can also be prepared by the staged deintercalation of Na^{1+} from NaCoO2 using I_2 in acetonitrile; however, the solid state method is more facile. The sodium cobaltates were stored in a glovebox to prevent hydrolysis over time from reaction with atmospheric water.

Synthesis of Ca_xCoO_2 phases The aliovalent exchange of calcium for sodium was completed by intimately mixing the sodium precursor with 4 equivalents of previously dried $Ca(NO_3)_2$ in a glovebox then firing the powder under O_2 for 48 hours at 310 °C. The reaction products were washed with water to remove the nitrate salts then dried under vacuum and stored in a nitrogen filled desiccator.

Calcium exchange phases containing Fe as the transition metal were synthesized similarly with one change – the calcium exchange was performed at 225 °C rather than 310 °C to avoid decomposition.

Synthesis of reduced oxidation state layered phases Topotactic chemical intercalation of Na and Li into the vacancies of the layered framework was performed using standard organometallic reducing agents at room temperature in the glove box. A 20 mL glass vial was charged with 250 mg of the calcium phase and 10 molar excess of either 1.6M nBuLi in hexanes or 1M Na-benzophenone in THF depending on the desired product, and a magnetic stir bar. The reaction was allowed to stir for up to 10 days depending on the phase and final composition desired (Table S2). After the reaction was complete the final products were washed with 5 20 mL aliquots of pentane for the Li intercalation or THF for the Na intercalation reactions to remove excess starting material.

Synthesis of Fe analogues $NaFeO_2$ was prepared by grinding 10g (62.6 mmol) Fe_2O_3 and 5.1g (125 mmol) NaOH under N_2, heating the mixture in an alumina boat to 330 °C over 5 hours, holding at 330 °C for 10 hours, then raising the temperature to 500 °C and firing for 48 hours under O_2. The product was washed with anhydrous ethanol under N_2 to remove excess NaOH.

Powder x-ray diffraction (PXD) patterns were obtained on a Bruker D2-Phaser diffractometer using Cu-K_α radiation (λ = 1.5418 Å), a 2mm beam slit, and a step size of 0.02° 2θ.

Inductively-Coupled Plasma Atomic Emission Spectroscopy (ICP-AES) was used to determine the elemental composition of the synthesized compounds. ICP-AES was performed on a Varian Vista-MPX CCD instrument. Standard solutions of 1 ppm, 10 ppm, and 100 ppm were prepared from stock solutions of 1000 ppm Li, Na, Ca, and Co salts obtained from Sigma Aldrich (Puratronic Tracert, standardized). Samples were run in quintuplicate to afford the emission intensity used to derive concentration from calibration curves of the standards.

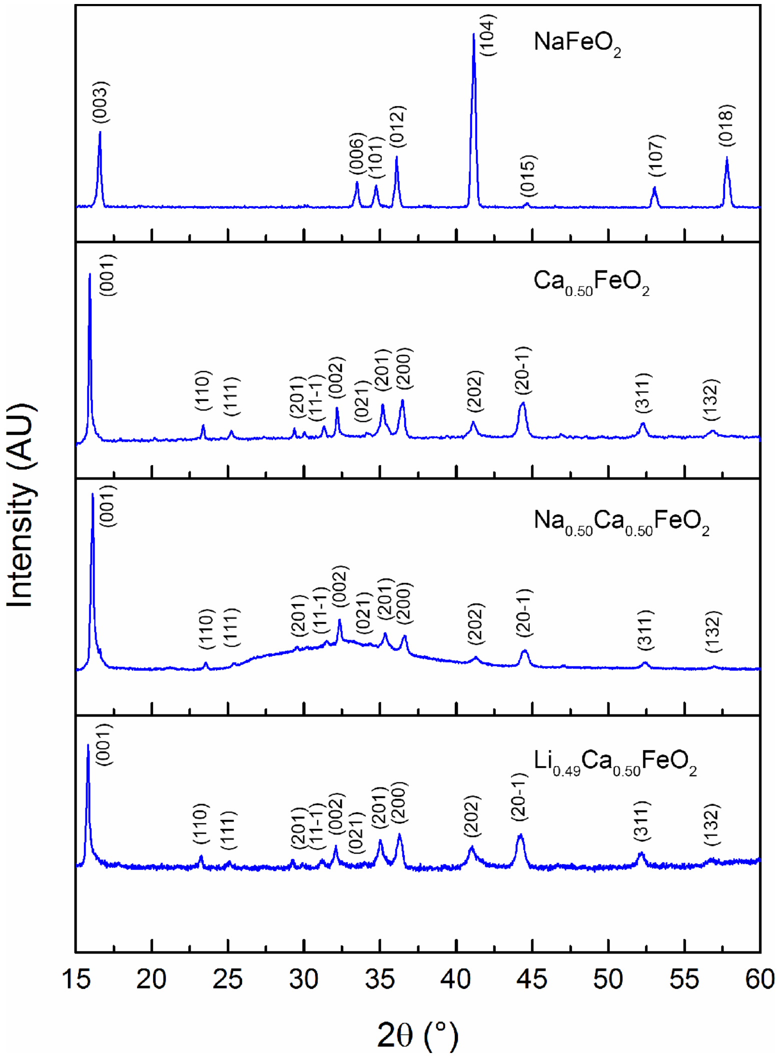

Figure S1. PXD patterns of the Fe species prepared using this novel multistep preparation method. Only the most intense peaks are labeled (for clarity) in the monoclinic $Ca_{0.5}FeO_2$, $Na_{0.50}Ca_{0.50}FeO_2$, and $Li_{0.49}Ca_{0.50}FeO_2$. Due to the extremely air and water sensitive nature of the final phases, patterns of the intercalated materials were obtained either using an air-free sample holder ($Na_{0.50}Ca_{0.50}FeO_2$) or a glass capillary ($Li_{0.49}Ca_{0.50}FeO_2$). Contribution from the sample holder is the reason for the unindexed peaks/amorphous background in $Na_{0.50}Ca_{0.50}FeO_2$.

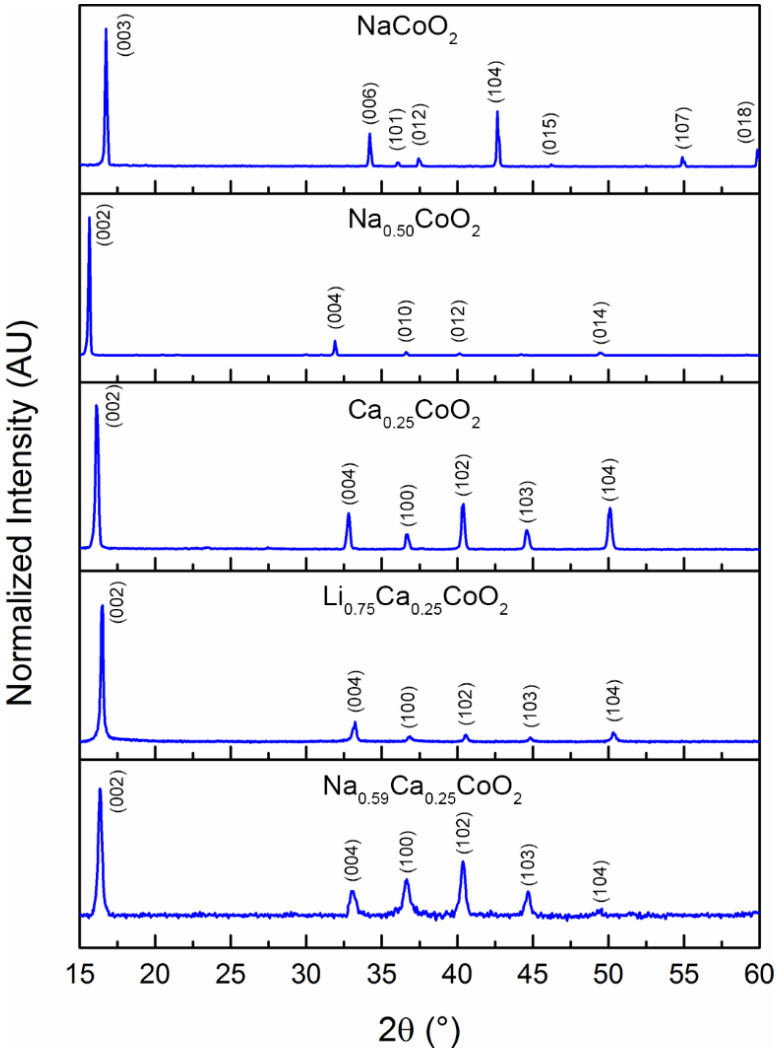

Figure S2. PXD patterns of the $A_xCa_{0.25}CoO_2$ family of materials using the multistep preparation method.

Particle Size Determination by Whole Powder Pattern Modeling (WPPM) Approach Using PM2K Software

WPPM is a powerful method that models a peak profile directly to extract microstructural and information from the entire pattern, rather than a subset, by combining pattern fitting techniques based on both integral breadth and Fourier methods [1–3]. Necessary parameters for the extraction of particle size from the powder diffraction pattern were obtained using the PM2K software suites [4]. The major assumptions using this modeling method include: minimum peak overlap in the diffraction pattern, high counting statistics, and a Lorentzian peak shape. A lognormal size distribution was used to calculate the particle size of the samples. There is precedence in the literature for the use of a lognormal distribution of particle sizes for particles used in different chemical methods, including catalysis [5].

The lognormal function employed for this size distribution study is a combination of the lognormal mean μ and the lognormal variance σ:

$$g_l(D) = \frac{1}{D\sigma(2\pi)^{1/2}} \exp(-\ln D - \mu)^2 / 2\sigma^2$$

where D is the diameter of the spherical particle. A more in-depth description of the lognormal function and the Fourier transform of said function that is used in the PM2K software suite is given by Scardi and Leoni [6].

The instrument profile component of the powder x-ray diffraction pattern was modeled with the Caglioti formula to parametize the FWHM and Lorentzian fractions [7]:

$$FWHM^2 = W + V\tan(\Theta) + U\tan^2(\Theta)$$

$$\eta_{Lorentz} = a + b\Theta_{\mathrm{deg}} + c\Theta_{\mathrm{deg}}^2$$

where θ is half of the Bragg angle 2θ. The W, V, U, a, b, and c parameters were refined by PM2K to optimize the Caglioti profile function then fixed as we assumed that the instrumental contribution is constant for the instrument and is not dependent on the sample [8].

Results from the WPPM analysis as well as SEM images of the particles are found in Table S1 and Figure S3, respectively.

Table S1. Particle size distributions obtained using the WPPM algorithms implemented in the PM2K software suite.[6] PM2K results gave the shortest length (height of platelet) for platelet type particles.

Material	Space Group	Cell Parameters (Å) (values for precursor phases from [9–11])	Particle Size (nm) from PM2K	Particle Size (nm) from SEM
$NaCoO_2$	$R\overline{3}m$	a = 2.886 c = 15.60	> 1 µm	-
$Ca_{0.50}CoO_2$	C2/m	a = 4.881 b = 2.826 c = 5.654 ß = 105.86 °	512 ± 95	-
$Li_{0.47}Ca_{0.50}CoO_2$	C2/m	a = 4.789(3) b = 4.027(5) c = 5.696(3) ß = 107.5(2) °	119 ± 12	-
$Na_{0.31}Ca_{0.50}CoO_2$	$R\overline{3}m$	a = 2.831(1) c = 16.288(3)	128 ± 21	-
$Na_{0.74}CoO_2$	$P6_3/mmc$	a = 2.843 c = 10.81	> 1 µm	900 - 1100
$Ca_{0.37}CoO_2$	$P6_3/mmc$	a = 2.812 c = 10.87	502 ± 259	650 - 725
$Li_{0.64}Ca_{0.37}CoO_2$	$P6_3/mmc$	a = 2.818(2) c = 10.820(6)	114 ± 52	-
$Na_{0.59}Ca_{0.37}CoO_2$	$P6_3/mmc$	a = 2.856(2) c = 10.809(3)	157 ± 17	148 - 205
$Na_{0.51}CoO_2$	$P6_3/mmc$	a = 2.820 c = 11.04	> 1 µm	-
$Ca_{0.25}CoO_2$	$P6_3/mmc$	a = 2.822 c = 10.91	800 ± 235	-
$Li_{0.75}Ca_{0.25}CoO_2$	$P6_3/mmc$	a = 2.817(4) c = 10.794(5)	130 ± 70	-
$Na_{0.67}Ca_{0.25}CoO_2$	$P6_3/mmc$	a = 2.828(6) c = 10.851(2)	143 ± 10	-
$NaFeO_2$	$R\overline{3}m$	a = 3.025 c = 16.047	> 1 µm	600 - 800
$Ca_{0.50}FeO_2$	C2/m	a = 5.174(1) b = 5.953(2) c = 5.821(3) ß = 73.21(2) °	> 1 µm	550 - 750
$Li_{0.49}Ca_{0.50}FeO_2$	C2/m	a = 5.173(4) b = 5.948(2) c = 5.804(1) ß = 73.12(4) °	117 ± 29	-
$Na_{0.50}Ca_{0.50}FeO_2$	C2/m	a = 5.179(6) b = 5.964(3) c = 5.802(1) ß = 73.24(1) °	514 ± 244	475 - 575

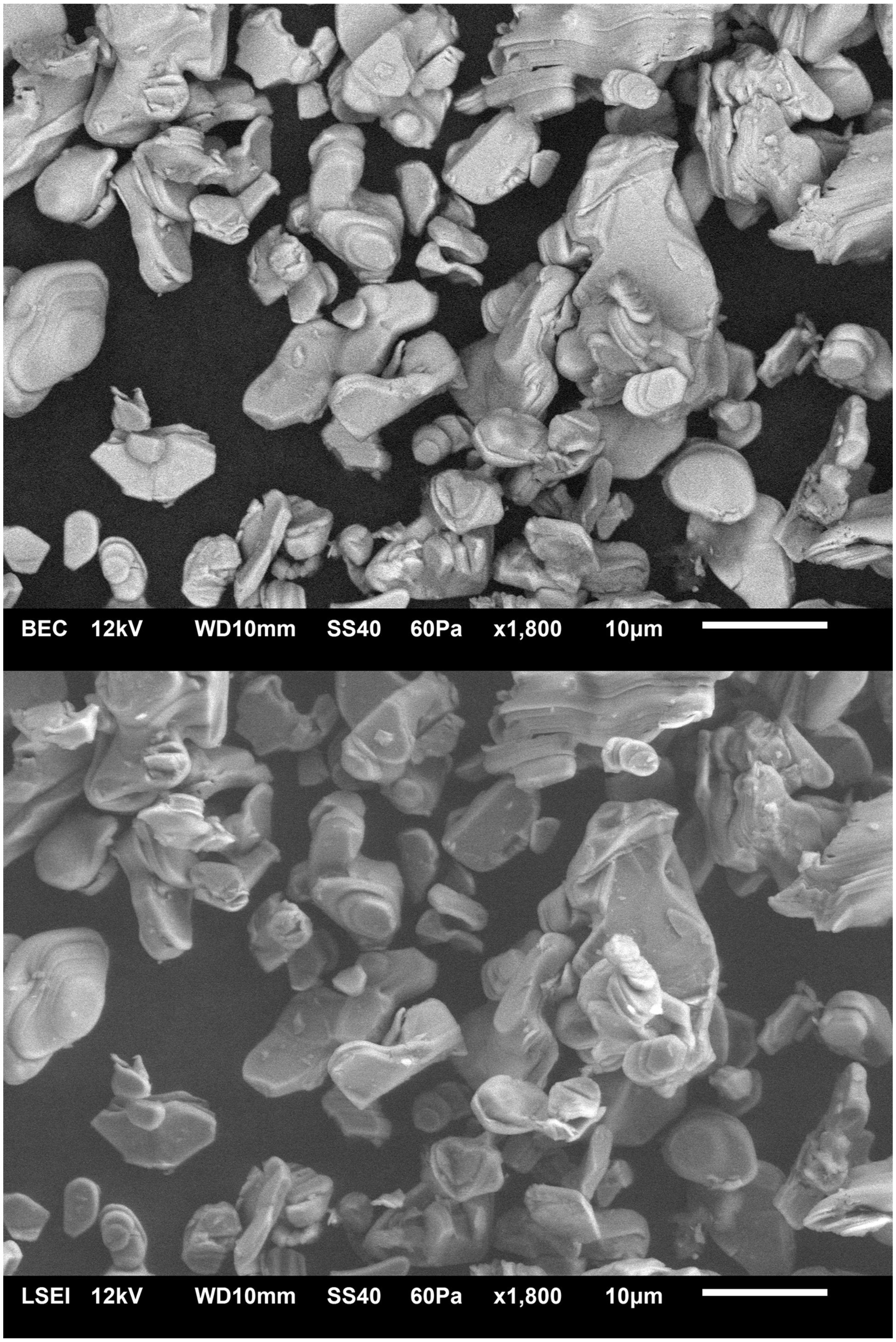

Figure S3. SEM image of $Na_{0.59}Ca_{0.37}CoO_2$ using back scattered electrons (top) and secondary electrons (bottom) showing the large anisotropy in crystal dimensions resulting in platelets. Clearly, the ridges on the larger particles are actually many different platelets stacked together.

Table S2. Compound stoichiometry over intercalation time for the preparation of the reduced phases presented in the manuscript. Generally, Li^{1+} intercalated phases were synthesized after stirring for 5 days while intercalation of the larger Na^{1+} ion warranted full 10 day reactions. Bolded numbers are stopping points for the preparation each compound. Iron containing phases were stirred for 120 hrs days regardless of alkali metal to achieve full intercalation.

Compound	**x (stoichiometry) after time (hrs)**					
	24	**48**	**72**	**96**	**120**	**240**
$Li_xCa_{0.50}CoO_2$	0.212	0.371	0.435	0.475	**0.489**	0.498
$Li_xCa_{0.37}CoO_2$	0.446	0.523	0.591	0.627	**0.642**	0.638
$Li_xCa_{0.25}CoO_2$	0.268	0.313	0.475	0.682	**0.751**	0.762
$Na_xCa_{0.50}CoO_2$	0.062	0.078	0.123	0.153	0.199	**0.313**
$Na_xCa_{0.37}CoO_2$	0.295	0.218	0.275	0.495	0.542	**0.593**
$Na_xCa_{0.25}CoO_2$	0.174	0.183	0.325	0.389	0.472	**0.665**

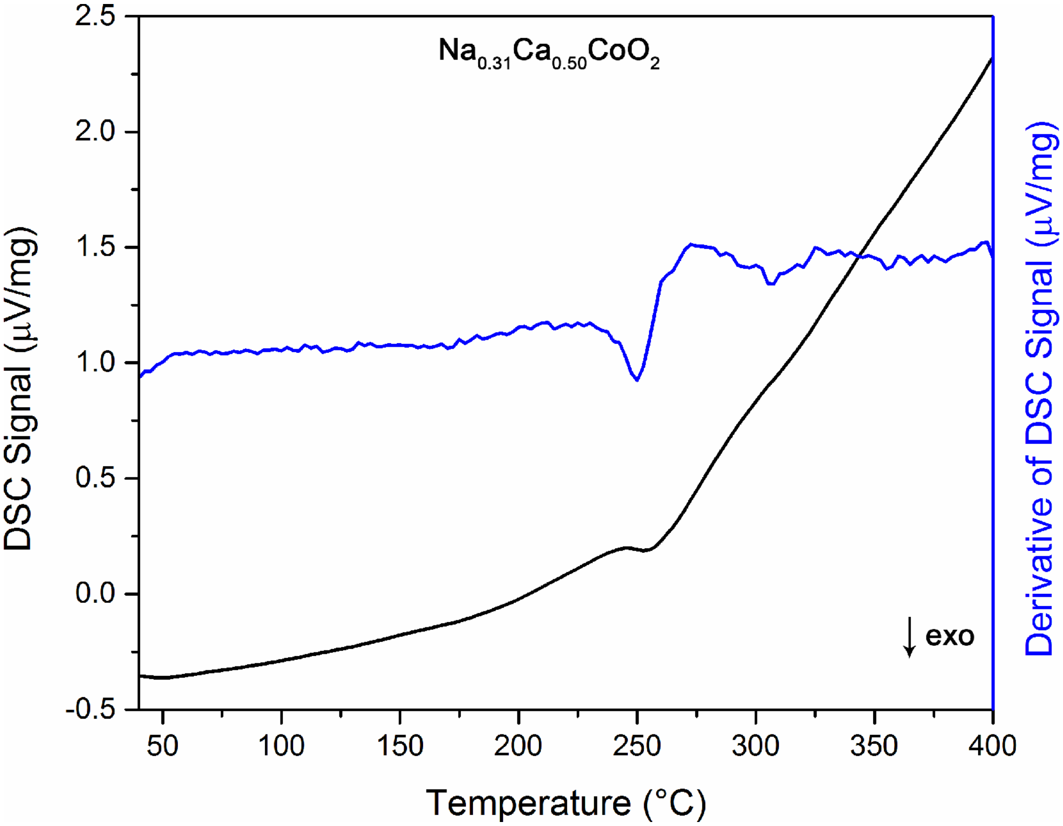

Figure S4. Differential scanning calorimetry trace of $Na_{0.31}Ca_{0.50}CoO_2$ with the first derivative of the trace. DSC curves of other materials prepared with this method are similar. Curves were corrected for instrumental noise using blank sample pans under the same experimental conditions.

Brief Discussion on the crystal structures with triangular (CdI_2-type) layers

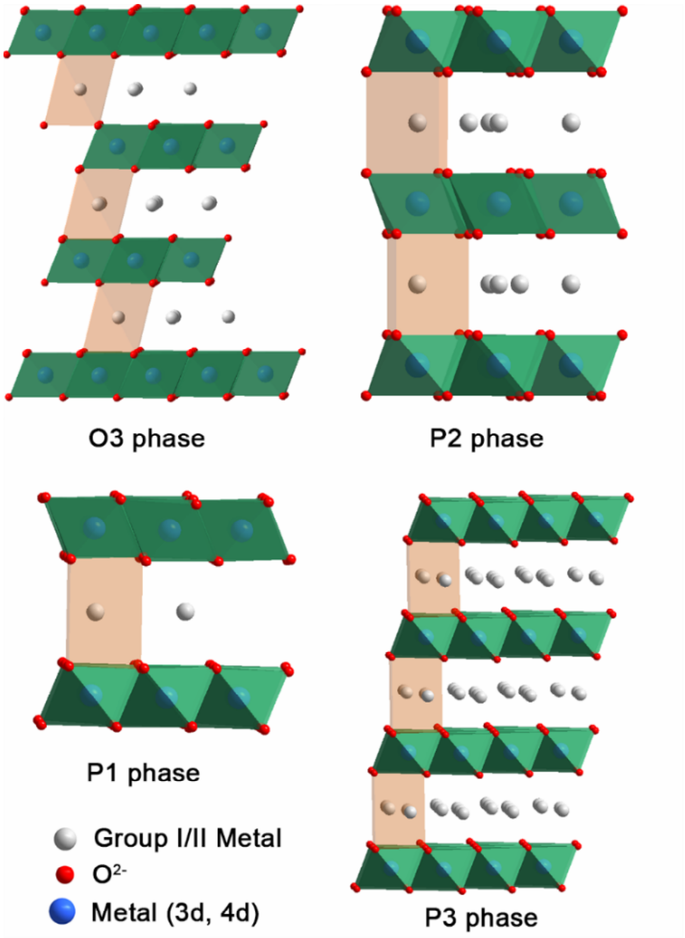

Figure S5. Different structure variations found in compounds with triangular (CdI_2-type) layers based on the coordination of the alkali metal – O for octahedral and P for trigonal prismatic – and the number of layers per primitive cell.

Originally presented by Delmas,[12] a simple hexagonal packing scheme with three distinct oxygen positions (A, B, C) can be used to identify the cation geometry between $(MO_2)_n$ sheets. Assuming the oxygen in the $(MO_2)_n$ sheets are in the A and B positions, only two possibilities exist for the position of the third oxygen sheet: B or C. When the third oxygen is located in the B position, either ABBA or ABBCCA stacking motifs can exist depending on the position of the fourth oxygen (either A or C, respectively), resulting in a trigonal prismatic coordination for the alkali metals between the $(MO_2)_n$ sheets. On the other hand, when the third oxygen is located on a C position an ABCABC stacking pattern is created with the alkali metals adopting octahedral symmetry. Once the geometry of the alkali cation is established - either O (octahedral) or P (trigonal prismatic) - the number of $(MO_2)_n$ repeating units per unit cell is appended to give the structural type. Finally, a prime is added after the geometry notation to inform of the presence of a monoclinic distortion of the unit cell.

In the multistep soft chemistry method presented in this communication, the structure of the precursor phase plays a determining role in the structure of the final phase. For all compounds derived from Na_1CoO_2 (O3) or $Na_{0.74}CoO_2$ (P2) the parent structure types are preserved. For example, in the $Na_{0.74}CoO_2 \rightarrow Ca_{0.37}CoO_2 \rightarrow A_xCa_{0.37}CoO_2$ phases, the P2 structural type is maintained throughout each intercalation step.

Supplemental Information References

S1. P. Scardi and M. Leoni, *Acta Crystallogr. Sect. A Found. Crystallogr.*, 2001, **57**, 604–613.

S2. J. Ahmed, C. K. Blakely, S. R. Bruno, and V. V. Poltavets, *Mater. Res. Bull.*, 2012, **47**, 2282–2287.

S3. C. K. Blakely, S. R. Bruno, Z. J. Baum, and V. V. Poltavets, *Solid State Sci.*, 2013, **15**, 110–114.

S4. M. Leoni, T. Confente, and P. Scardi, *Zeitschrift für Krist. Suppl.*, 2006, **2006**, 249–254.

S5. S. Hodjati, K. Vaezzadeh, C. Petit, V. Pitchon, and a Kiennemann, *Catal. Today*, 2000, **59**, 323–334.

S6. M. Leoni and P. Scardi, *J. Appl. Crystallogr.*, 2004, **37**, 629–634.

S7. G. Caglioti, A. Paoletti, and F. P. Ricci, *Nucl. Instruments*, 1958, **3**, 223–228.

S8. E. J. Mittemeijer and P. Scardi, Eds., *Diffraction Analysis of the Microstructure of Materials*, Springer Berlin Heidelberg, Berlin, Heidelberg, 2004, vol. 68.

S9. B. L. Cushing and J. B. Wiley, *J. Solid State Chem.*, 1998, **391**, 385–391.

S10. M. Foo, Y. Wang, S. Watauchi, H. Zandbergen, T. He, R. Cava, and N. Ong, *Phys. Rev. Lett.*, 2004, **92**, 1–4.

S11. B. L. Cushing, A. U. Falster, W. B. Simmons, and J. B. Wiley, *Chem Comm*, 1996, **2**, 2635–2636.

S12. C. Delmas, A. Maazaz, C. Fouassier, J.-M. Reau, and P. Hagenmuller, *Mater. Res. Bull.*, 1979, **14**, 329–335.